Journal of Computational Physics 368 (2018) 115–130

Contents lists available at ScienceDirect

Journal of Computational Physics

www.elsevier.com/locate/jcp

The stabilization of high-order multistep schemes for the Laguerre one-way wave equation solver

Andrew V. Terekhov

Institute of Computational Mathematics and Mathematical Geophysics, 630090, Novosibirsk, Russia

ARTICLE INFO

Article history:
Received 7 September 2017
Received in revised form 29 April 2018
Accepted 30 April 2018
Available online 4 May 2018

Keywords:
One-way wave equation
Finite difference method
Acoustic waves
Predictor–corrector
Adams–Moulton schemes

ABSTRACT

This paper considers spectral-finite difference methods of a high-order of accuracy for solving the one-way wave equation using the Laguerre integral transform with respect to time as the base. In order to provide a high spatial accuracy and stability, the Richardson method can be employed. However such an approach requires high computer costs, therefore we consider alternative algorithms based on the Adams multistep schemes. To reach the stability for the one-way equation, the stabilizing procedures using the spline interpolation were developed. This made it possible to efficiently implement a predictor–corrector type method thus decreasing computer costs. The stability and accuracy of the procedures proposed have been studied, based on the implementation of the migration algorithm within a problem of seismic prospecting.

1. Introduction

Mathematical models based on the one-way wave equation (OWWE) are often considered in problems of ocean acoustics [1–3], seismic prospecting [4–7], as well as for setting non-reflecting boundary conditions [8–10]

$$\frac{\partial \tilde{u}}{\partial z} = -\mathrm{i}\frac{\omega}{c}\sqrt{1-\left(\frac{ck_x}{\omega}\right)^2}\,\tilde{u}, \tag{1}$$

where $\mathrm{i} = \sqrt{-1}$, $\tilde{u} \equiv \tilde{u}(k_x, z, \omega)$ is a wave component at the angular frequency ω, k_x is the horizontal wave number, c is the wave velocity, the vertical direction z is the extrapolation direction, i.e., the direction of one-way propagation, and the positive axis z is directed downward, i.e., toward increasing depth. The square-root operator can be formally represented by the Padé expansion [11–14]

$$\sqrt{1-\left(\frac{ck_x}{\omega}\right)^2} \approx \left[1-\sum_{s=1}^{n}\frac{\beta_s c^2 k_x^2}{\omega^2-\gamma_s c^2 k_x^2}\right], \tag{2}$$

where the coefficients γ_s, β_s for the propagation angle should be optimized [12,15]. The velocity model is assumed to be homogeneous, although it yields satisfactory results also for inhomogeneous media. In the latter case this model correctly keeps kinematics of waves, but not their amplitudes.

E-mail address: andrew.terekhov@mail.ru.

https://doi.org/10.1016/j.jcp.2018.04.059
0021-9991/

The fundamental problem of the downward continuation algorithms of wave fields is the instability. If the coefficients γ_s, β_s are real, then for the angles around $\pi/2$ the argument of the square root becomes less than zero, the left-hand side of approximation (2) being complex, while the right-hand side is still real, hence causing inconsistency in the approximation. This results in an improper propagation of the evanescent mode which should exponentially decay. For stabilizing the real Padé approximation there are a few approaches [16–18] that allow suppressing unstable components of a wave field. On the other hand, setting the coefficients γ_s, β_s to be complex [19–22], a better consistency of the right-hand and the left-hand sides of approximation (2) can be attained. From the physical viewpoint this means the introduction of artificial dissipation that restricts an increase in instability for evanescent waves. However the presence of strong gradients of the velocity function, the use of the Marchuk–Strang type splitting for decreasing computer costs [23–25] and the simulation of high-frequency wave fields, can bring about the numerical instability. This is explained by the fact that optimal values of the coefficients γ_s, β_s are selected based on the principle of frozen coefficients for a homogeneous medium, while calculations are carried out for inhomogeneous velocity models with difference approximations and different decompositions for differential equations.

In addition to the problem of stability, one of the central computational problems of finite difference methods for solving equations (1), (2) is the inversion of the ill-conditioned systems of linear algebraic equations (SLAEs). For the two-dimensional problems direct methods for solving the SLAEs are rather efficient, but for the three-dimensional problems one has to use iterative procedures [26–28], which, as a rule, have low convergence rate for indefinite non-Hermitian matrices [29]. Direct methods for solving the SLAEs can be used for three-dimensional geometry. However, practical calculations show [30,31] that the number of mesh nodes has to be very small to calculate in a reasonable time.

To overcome these difficulties, a new approach to solving the problem (1), (2) was proposed in [32]. The solution is sought for as a series in Laguerre functions [33,34], while to increase the accuracy of spatial approximation the Richardson extrapolation [35] and dispersion-relation-preserving (DRP) schemes [36] are used. The coefficients of the Laguerre series expansion are recurrence relations and, therefore, can be calculated by solving the SLAEs with the same real well-conditioned matrix and different right-hand sides. To solve these SLAEs, it may be efficient to use the parallel dichotomy algorithm [37–39] in the two-dimensional case, and any iterative algorithm for positive-definite matrices in the three-dimensional case. In contrast to the Laguerre transform, the Fourier transform leads to SLAEs comprised of ill-conditioned matrices with complex entries. Another advantage of the algorithm [32] is that by combining the Laguerre transform with the Richardson method one can obtain a stable difference model of high-order accuracy and, at the same time, limit the growth of unstable harmonics when using the real Padé approximation of the operator (2).

Higher efficiency of calculations can be attained if one, instead of solving difference problems for the elliptic high-order operators, solves a sequence of problems for a second order operator, thereby decreasing the condition numbers of the SLAEs. For this we will consider a new method of the predictor–corrector type [40] based on multistep Adams finite difference schemes. Another feature of the algorithm proposed in the present paper is that higher accuracy of calculations is provided by using schemes of high approximation order, not by the Richardson extrapolation procedure, which increases the approximation order from second to fourth. However, it requires solving the initial equations on an auxiliary mesh with a doubled number of nodes. Unfortunately, practical calculations with multistep Adams schemes have shown that not only explicit but also implicit schemes of high-order accuracy forming the basis of the predictor–corrector method are unstable. To make the calculations stable, a new stabilizing algorithm based on spline filtering is proposed. It makes it possible to suppress instability of both the real Padé approximation (2) and the multistep schemes. Thus, the algorithm being proposed for solving the OWWE equation is computationally more efficient and has an order of accuracy that is higher than that of the method in [32], and its software implementation is easier and, hence, more efficient.

2. The stability analysis for a model 1D one-way wave equation

The aspects of stability in constructing a numerical method for solving the 2D OWWE occupy a highly important place. To investigate the stability let us first consider a model problem for the 1D OWWE:

$$\partial_t v + c\partial_x v = 0, \quad t > 0,\ x \in \mathbb{R} \tag{3}$$

with the initial condition $v(x,0) = \varphi(x),\ (\varphi(0) = \varphi(1))$ and the periodic boundary condition $v(0,t) = v(1,t)$.

To solve problem (3), let us consider the direct and inverse Laguerre transforms [34] of a function $g(t) \in L_2(0,\infty)$

$$\mathbb{L}\{g(t)\} = \bar{g}_m = \int_0^\infty g(t) l_m(\eta t) dt, \qquad g(t) = \mathbb{L}^{-1}\{\bar{g}_m\} = \sum_{m=0}^{\infty} \bar{g}_m l_m(\eta t), \tag{4}$$

where $l_m(\eta t) \equiv \sqrt{\eta}\exp(-\eta t/2) L_m(\eta t)$ are the orthogonal Laguerre functions, $L_m(t)$ is the Laguerre polynomial of m degree and $\eta > 0$ is the transformation parameter. Setting $\lim_{t\to\infty} g(t) = 0$, the following relations are valid [34,41]

$$\mathbb{L}\left\{\frac{d}{dt} g(t)\right\} = \frac{\eta}{2}\bar{g}_m + \Phi_1(\bar{g}_m), \tag{5}$$

where

$$\Phi_1(\bar{g}_m) = \sqrt{\eta} g(0) + \eta \sum_{j=0}^{m-1} \bar{g}_j. \tag{6}$$

Making use of transform (4) for equation (3), we obtain

$$\left(\frac{\eta}{2} + c\partial_x\right) \bar{v}^m + \Phi_1(\bar{v}^m) = 0,\ m = 0, 1, ..., \tag{7}$$

where the index m denotes number of a term in series (4). Taking into consideration

$$\Phi_1(\bar{v}^m) = \eta \bar{v}^{m-1} + \Phi_1(\bar{v}^{m-1}),$$

for studying the stability of difference schemes, let us turn to another form of equation (7):

$$\begin{cases} \left(c\partial_x + \dfrac{\eta}{2}\right) \bar{v}^0 + \sqrt{\eta}\varphi(x) = 0, & \text{(a)} \\ \left(c\partial_x + \dfrac{\eta}{2}\right) \bar{v}^m = \left(c\partial_x - \dfrac{\eta}{2}\right) \bar{v}^{m-1},\ m = 1, 2, ... & \text{(b)} \end{cases} \tag{8}$$

For solving (8b) let us consider the difference scheme of the first order of accuracy

$$\frac{c\left(\bar{v}^m_{j+1} - \bar{v}^m_j\right)}{h_x} + \frac{\eta}{2}\bar{v}^m_j = \frac{c\left(\bar{v}^{m-1}_{j+1} - \bar{v}^{m-1}_j\right)}{h_x} - \frac{\eta}{2}\bar{v}^{m-1}_j. \tag{9}$$

Substituting the solution in the form $\bar{v}^m_j = \tilde{\bar{v}}^m \exp(\mathrm{i}k_x j h_x)$ into difference equation (9), obtain

$$\tilde{\bar{v}}^m = \frac{\exp(\mathrm{i}k_x h_x) - \beta - 1}{\exp(\mathrm{i}k_x h_x) + \beta - 1} \tilde{\bar{v}}^{m-1} = G(k_x)\tilde{\bar{v}}^{m-1}. \tag{10}$$

Here $\beta = \eta h_x/(2c)$; $G = G(k_x)$ is called the amplification factor which is a complex function of the wavenumber k_x. A difference equation will be stable in the Von Neumann sense [42] if $|G(k_x)| \le 1\ \forall\ k_x$. For equation (10) let us estimate the value

$$|G(k_x)|^2 = \frac{(\beta + 1 - \cos(k_x h_x))^2 + \sin^2(k_x h_x)}{(\beta - 1 + \cos(k_x h_x))^2 + \sin^2(k_x h_x)} = \frac{A^2}{B^2}. \tag{11}$$

For $c > 0$, obtain $A^2 - B^2 = 4\beta(1 - \cos(k_x h_x)) \ge 0$, hence, $|G(k_x)|^2 \ge 1$ and scheme (9) will be unstable. For $c < 0$ it can be shown that $|G(k_x)|^2 \le 1$, which suggests the stability of the scheme.

Now let us consider another method of the first order of accuracy

$$\frac{c\left(\bar{v}^m_{j+1} - \bar{v}^m_j\right)}{h_x} + \frac{\eta}{2}\bar{v}^m_{j+1} = \frac{c\left(\bar{v}^{m-1}_{j+1} - \bar{v}^{m-1}_j\right)}{h_x} - \frac{\eta}{2}\bar{v}^{m-1}_{j+1}. \tag{12}$$

In a similar manner reducing scheme (12) to the form $\tilde{\bar{v}}^m = G(k_x)\tilde{\bar{v}}^{m-1}$, we obtain that for $c > 0$ the value $A^2 - B^2 = 4\beta(\cos(k_x h_x) - 1) \le 0$ and, hence, $|G(k_x)|^2 \le 1$. Thus, scheme (12) will be stable for $c > 0$ and unstable for $c < 0$.

Let us consider the Crank–Nicolson scheme (CN-Scheme) [43] of the second order of accuracy

$$\frac{c\left(\bar{v}^m_{j+1} - \bar{v}^m_j\right)}{h_x} + \frac{\eta}{4}\left(\bar{v}^m_{j+1} + \bar{v}^m_j\right) = \frac{c\left(\bar{v}^{m-1}_{j+1} - \bar{v}^{m-1}_j\right)}{h_x} - \frac{\eta}{4}\left(\bar{v}^{m-1}_{j+1} + \bar{v}^{m-1}_j\right). \tag{13}$$

It is not difficult to obtain that for the scheme in question $|G(k_x)| = 1$ holds, therefore scheme (13) is unconditionally stable.

Let us consider finite difference approximations for equation (8b) based on the Adams–Moulton scheme (AM-Scheme) [40]

$$c\frac{\bar{v}^m_{i+1} - \bar{v}^m_i}{h_x} + \frac{\eta}{2\varrho}\sum_{j=-3}^{1} \alpha_j \bar{v}^m_{i+j} = c\frac{\bar{v}^{m-1}_{i+1} - \bar{v}^{m-1}_i}{h_x} - \frac{\eta}{2\varrho}\sum_{j=-3}^{1} \alpha_j \bar{v}^{m-1}_{i+j}. \tag{14}$$

To begin with, we investigate the stability of the third order accuracy scheme for which the coefficients are equal to $\varrho = 12$, $\alpha_{-3} = 0$, $\alpha_{-2} = 0$, $\alpha_{-1} = -1$, $\alpha_0 = 8$, $\alpha_1 = 5$. Substituting the solution in the form $\bar{v}^m_j = \tilde{\bar{v}}^m \exp(\mathrm{i}k_x j h_x)$ into (14), obtain

$$\tilde{\bar{v}}^m = G(k_x)\tilde{\bar{v}}^{m-1} = \frac{-\beta(5\exp(2\mathrm{i}k_x h_x) + 8\exp(\mathrm{i}k_x h_x) - 1) + \exp(2\mathrm{i}k_x h_x) - \exp(\mathrm{i}k_x h_x)}{\beta(5\exp(2\mathrm{i}k_x h_x) + 8\exp(\mathrm{i}k_x h_x) - 1) + \exp(2\mathrm{i}k_x h_x) - \exp(\mathrm{i}k_x h_x)},$$

where $\beta = \frac{\eta h_x}{2c\rho}$.

Whence it follows that $|G(k_x)|^2 = \frac{A^2}{B^2}$, where

$$A^2 = \left(-20\beta^2 + 4\beta\right)(\cos(k_x h_x))^2 + \left(64\beta^2 - 8\beta - 2\right)\cos(k_x h_x) + 100\beta^2 + 4\beta + 2,$$
$$B^2 = \left(-20\beta^2 - 4\beta\right)(\cos(k_x h_x))^2 + \left(64\beta^2 + 8\beta - 2\right)\cos(k_x h_x) + 100\beta^2 - 4\beta + 2.$$

Then for $c > 0$ from $A^2 - B^2 = 8\beta(\cos(k_x h_x) - 1)^2 \geq 0$ it follows that $|G(k_x)|^2 \geq 1$, hence, the third order scheme is unstable, while for $c < 0$ the scheme is stable.

The coefficients of the fourth order scheme are equal to $\varrho = 24$, $\alpha_{-3} = 0$, $\alpha_{-2} = 1$, $\alpha_{-1} = -5$, $\alpha_0 = 19$, $\alpha_1 = 9$ and $A^2 - B^2 = -16\beta(\cos(k_x h_x) - 1)^3$, whence follows the instability of scheme (14) for $c > 0$ and the stability for $c < 0$.

The coefficients of the fifth order scheme are equal to $\varrho = 720$, $\alpha_{-3} = -19$, $\alpha_{-2} = 106$, $\alpha_{-1} = -264$, $\alpha_0 = 646$, $\alpha_1 = 251$, for which we obtain

$$A^2 - B^2 = -16\beta\left(38\cos(k_x h_x) - 11\right)(\cos(k_x h_x) - 1)^3.$$

Depending on the wavenumber k_x, the latter formula can take both positive and negative values. Thus, the amplification factor $|G(k_x)|$ is not limited by the unit, therefore the fifth order scheme is unstable.

To conclude, for solving 2d OWWE in the context of the Laguerre method the AM-scheme of the form of (14) cannot be used due to its absolute instability for $c > 0$. To overcome these difficulties we will consider the ways of stabilizing the multistep AM-schemes of a high-order of accuracy first for the 1D and then for the 2D OWWE.

3. The stabilization of high-order schemes for the 1D one-way wave equation

For equation (3) at $c > 0$ instead of the periodic boundary conditions we consider the initial and boundary conditions of the form:

$$\begin{aligned} &v(0,t) = f(t), \quad t \geq 0, \\ &v(x,0) = 0, \qquad x \geq 0, \\ &f(0) = 0. \end{aligned} \tag{15}$$

A stable spectral-finite difference algorithm for solving the 2D OWWE was proposed in [32]. It includes the Richardson extrapolation procedure that for problem (7), (15) and scheme (13) can be written down in the following form.

Algorithm 1-1. The Richardson extrapolation. Let the auxiliary functions $\bar{v}^m(\Omega_1)$, $\bar{v}^m(\Omega_2)$ be defined on the meshes Ω_1, Ω_2 with the mesh steps h_x and $h_x/2$. To calculate the functions $\bar{v}^m$ accurate to $O(h_x^4)$, the following is necessary:

1. Based on the cubic splines interpolate values of the function $\Phi_1(\bar{v}^m)$, preset on the mesh Ω_1, into nodes Ω_2.
2. On the mesh Ω_1, applying equation (13), calculate the solution $\bar{v}^m(\Omega_1)$.
3. On the mesh Ω_2, applying equation (13), calculate the solution $\bar{v}^m(\Omega_2)$.
4. Based on the Richardson extrapolation, correct the mesh function with the following:

$$\bar{v}^m = \frac{1}{3}\left(4\bar{v}^m(\Omega_2) - \bar{v}^m(\Omega_1)\right).$$

5. Turn to the calculation of the $(m+1)$th, the $(m+2)$th, etc. coefficients of the expansion of the Laguerre series.

This technique of calculating the Laguerre series coefficients is stable and provides the fourth order of accuracy [32]. However the necessity of calculating $\bar{v}^m(\Omega_2)$ triples the common computer costs, therefore there arises a problem of constructing a more efficient method of no less than fourth order of accuracy. Let us consider a difference approximation for equation (7) based on the Adams–Moulton multistep method of the fifth order of accuracy

$$c\frac{\bar{v}^m_{i+1} - \bar{v}^m_i}{h_x} = -\frac{1}{720}\sum_{j=-3}^{1}\alpha_j\left(\frac{\eta}{2}\bar{v}^m_{i+j} + \Phi_1\left(\bar{v}^m_{i+j}\right)\right), \tag{16}$$

where the coefficients of the difference scheme are equal to $\alpha_{-3} = -19$, $\alpha_{-2} = 106$, $\alpha_{-1} = -264$, $\alpha_0 = 646$, $\alpha_1 = 251$. As has been proven above, the fifth order AM-Scheme (14) or its equivalent form (16) is unstable according to the Von Neumann spectral property, but it can be stabilized when carrying out calculations in the following manner.

Algorithm 1-2. The stabilization of the Adams–Moulton scheme via the quintic spline filtration.

To calculate the functions $\bar{v}^m$ accurate to $O(h_x^5)$ on the mesh Ω with the mesh step h_x, the following is necessary:

1. Let the number of nodes of the mesh Ω be odd. Construct the quintic splines [44] for the function $\Phi_1(\bar{v}^m)$ using only odd nodes of the mesh.
2. Replace values of the function $\Phi_1(\bar{v}^m_k)$ for even k by their interpolated values (the quintic spline filtration).

3. Applying equation (16), calculate the solution $\bar{v}^m$.
4. Turn to the calculation of the $(m+1)$th, the $(m+2)$th, etc. coefficients of the expansion of the Laguerre series.

As will be shown in Section 5, such a calculation algorithm makes it possible to stabilize the numerical instability of scheme (16) and to attain a higher approximation order as compared to the Richardson extrapolation. To stabilize the solution, instead of the quintic spline [44] one can use other interpolation algorithms [45,46]: the cubic spline interpolation, barycentric, Lagrangian, etc. However numerous computer-aided experiments have not revealed any advantages over splines because the procedures of constructing the splines are efficient enough as compared to solving the elliptic equations in the 2D case. In addition, the barycentric interpolation demands high computer costs and both the Lagrangian interpolation and the cubic spline-interpolation are more dissipative than the quintic splines. If splines are not being used, the nodes of an interpolating polynomial should be symmetrically placed regarding the node for which the interpolated value is calculated. Otherwise due to the asymmetry of interpolation nodes the profile of a wave is distorted or the instability of calculation arises.

We can offer another way of stabilizing the numerical instability of the AM-schemes, which does not demand the calculation of splines.

Algorithm 1-3. The stabilization of the Adams–Moulton scheme via inconsistent approximation.

1. Taking into account the equivalence of problems (7) and (8), for computing the values of the grid functions $\Phi_1\left(\bar{v}_i^m\right)$ instead of (6) use the following approximation

$$\Phi_1\left(\bar{v}_i^m\right) = -\frac{\eta}{2}\bar{v}_i^{m-1} + c\frac{-\bar{v}_{i+2}^{m-1} + 8\bar{v}_{i+1}^{m-1} - 8\bar{v}_{i-1}^{m-1} + \bar{v}_{i-2}^{m-1}}{12h_x} + O\left(h_x^4\right). \tag{17}$$

2. Solve equation (7) through scheme (16).
3. Turn to the calculation of the $(m+1)$th, the $(m+2)$th, etc. coefficients of the expansion of the Laguerre series.

The non-consistent approximation of the operator $\partial/\partial x$ for the right-and the left-hand sides of equations (7), (8), stipulates supplementary non-physical dissipation preventing the development of instability. In this case, if instead of the central approximation of the fourth order of accuracy in (17) one uses a higher order approximation or a non-central scheme, the stability is lost.

Thus, in addition to the Richardson method, other stable algorithms of a high-order of accuracy can be proposed. However for calculating the value $\bar{v}^m$, the function $\bar{v}^{m-1}$ should be known throughout the whole calculation domain as its values are needed for implementing the stabilizing procedures.

4. The analytical solution via the Laguerre transforms for the 1D one-way wave equation

In order to assess the accuracy of the algorithms proposed, let us consider a fully analytical method for solving the 1D OWWE. To satisfy boundary conditions (15), we seek the solution to equation (8) in the form

$$\bar{v}^m(x) = \sum_{j=0}^{\infty} V_j^m l_j(\kappa x), \quad m = 0, 1, 2..., \tag{18}$$

where the transformation parameter $\kappa > 0$. Then, after applying the Laguerre spatial transform to equation (8) with allowance for initial boundary conditions (15) we have

$$\begin{cases} (\eta + c\kappa)\, V_0^m = (-\eta + c\kappa)\, V_0^{m-1} + 2c\sqrt{\kappa}\left(\bar{f}^m - \bar{f}^{m-1}\right), & m = 0, 1, ..., \quad \text{(a)} \\ (\eta + c\kappa)\, V_j^m + 2c\Upsilon(V_j^m) = (-\eta + c\kappa)\, V_j^{m-1} + 2c\Upsilon(V_j^{m-1}), & m = 0, 1, ...;\ j = 1, 2, .., \quad \text{(b)} \end{cases} \tag{19}$$

where

$$\Upsilon\left(V_j^m\right) = \kappa \sum_{i=0}^{j-1} V_i^m = \kappa V_{j-1}^m + \Upsilon\left(V_{j-1}^m\right), \tag{20}$$

$$V_j^m \equiv 0,\ \bar{f}^m \equiv 0, \quad \forall\, m < 0.$$

Taking (20) into account, equation (19b) takes the following form

$$(\eta + c\kappa)\, V_j^m + (\eta - c\kappa)\, V_j^{m-1} = (\eta - c\kappa)\, V_{j-1}^m + (\eta + c\kappa)\, V_{j-1}^{m-1}, \quad m = 0, 1, ...;\ j = 1, 2, ... \tag{21}$$

Since $c > 0$, then selecting $\kappa = \eta/c$, we finally obtain

Table 1
Dependence of the error value $\varepsilon = \|u^{\text{exact}} - u^h\|_2 / \|u^{\text{exact}}\|_2$ on the number of mesh nodes for different methods. Here p is the observed order of accuracy calculated according to Runge's rule at each level of grid refinement.

N_x	AM5-I5		AM6-I7		CN		RK4		Richardson		AM5-D4	
	ε	p	ε	p	ε	p	ε	p	ε	p	ε	p
1000	0.32	–	0.18	–	1.51	–	0.99	–	6.04e-2	–	0.56	–
1500	6.67e-2	3.86	2.4e-2	4.96	1.47	0.06	0.92	0.18	1.13e-2	4.13	0.18	2.8
2000	1.72e-2	3.34	4.6e-3	5.74	1.38	0.21	0.6	1.48	3.5e-3	4.07	6.5e-2	3.54
3000	2.3e-3	4.96	4.18e-4	5.91	0.87	0.13	0.16	3.25	6.82e-4	4.03	1.33e-2	3.91
4000	5.6e-4	4.91	7.52e-5	5.96	0.53	1.72	5.46e-2	3.73	2.14e-4	4.02	4.2e-3	4.01
4500	3.1e-4	5.02	3.72e-5	5.97	0.43	1.77	3.39e-2	4.04	1.33e-4	4.03	2.6e-3	4.07

$$\begin{cases} V_0^m = \kappa^{-1/2}\left(\bar{f}^m - \bar{f}^{m-1}\right), & m = 0, 1, ..., \\ V_j^m = V_{j-1}^{m-1}, & m = 0, 1, ...;\ j = 1, 2, ... \end{cases} \tag{22}$$

Based on (18), (22), we can write down the solution to equation (8), (15) in the form

$$\bar{v}^m(x) = \sum_{j=0}^{\infty} V_j^m l_j(\kappa x) = \sum_{j=0}^{m} V_0^{m-j} l_j(\kappa x), \quad m = 0, 1, 2, ... \tag{23}$$

The latter sum in (23) is a discrete linear convolution, therefore for a given x the functions $\bar{v}^m(x)$, $m = 0, ..., M$ can be computed in $O(M \log M)$ arithmetical operations based on the FFT algorithm [47]. Note that if we select $\kappa \neq \eta/c$, the solution for $\bar{v}^m$ will not be representative in the form of convolution thus increasing computer costs. The final solution to equation (3) in the time domain is calculated via the inverse Laguerre transform (4). Operational properties of the Laguerre series are also discussed in [48,49].

5. Numerical experiments for the 1D one-way wave equation

For testing the methods proposed for solving the 1D OWWE, we used a homogeneous medium model with the velocity 3000 m/s. For the test calculations we set boundary condition (15) depending on time as

$$f(t) = \exp\left[-\frac{(2\pi f_0(t - t_0))^2}{\delta^2}\right] \sin(2\pi f_0(t - t_0)), \tag{24}$$

where $t_0 = 0.2s$, $\delta = 4$, $f_0 = 30$Hz. As compared to the Fourier transform, where the basis functions are uniquely defined, for using the Laguerre transform (4) the parameter η should be set. This parameter was experimentally chosen by analyzing the convergence rate of the Fourier–Laguerre series for the shifted function $f(t)$ with $t_0 = T$, where T is the upper boundary of the time interval for which the wave field is calculated. The parameter η is chosen so that the function f(t) with $t_0 = T$ in the mean-quadratic norm be approximated accurate to $\varepsilon < 10^{-10}$. The number of addends in series (4) is $n = 2500$ for $T = 2$ s; the expansion parameter is $\eta = 600$.

From Table 1 it is evident that with decreasing the mesh size by a factor of two, the error of the Adams and the Richardson methods is decreasing according to the theoretical approximation order. For example, for the meshes with the number of nodes $N_x = 2000$ and $N_x = 4000$ the values of the error of the AM-scheme of the fifth order with the quintic spline interpolation (AM5-I5) has 31 times difference, which almost corresponds to the fifth order of approximation. The AM-scheme of the sixth order with the seventh order spline interpolation (AM6-I7) demonstrates the sixth order of approximation, while the AM-scheme of the fifth order and formula (17) (AM5-D4) is only of the fourth order of approximation.

From Table 1 and Fig. 1 it also follows that for certain values of N_x, the Richardson extrapolation of the fourth order of approximation is more accurate as compared to the Adams methods of the fifth and sixth orders. There is no contradiction because the estimation of the accuracy of difference schemes includes a constant independent of the mesh size. This constant is smaller for the Richardson method as compared to the AM5-15 method as the splines are constructed on the mesh with a doubled step. However, the fifth and six order methods have a higher rate of convergence as compared the Richardson method. Beginning with a certain mesh step they demonstrate a higher accuracy.

In addition, the Richardson method requires the solution to the supplementary problem on the mesh Ω_2, therefore it is more correct to compare the accuracy of calculations when the general number of nodes of the meshes Ω_1, Ω_2 is equal to the number of nodes of the mesh Ω for other methods. Indeed, comparing solutions for the Richardson method with $N_x = 1500$ for the mesh Ω_1 and the Adams methods with $N_x = 4500$, it is evident (Table 1) that the latter are significantly more accurate. Applying the spline-filtration procedure does not bring about a considerable loss in accuracy, otherwise the accuracy of the methods AM5-I5, AM6-I7 would be lower or compatible with the fourth order method AM5-D4, for which the filtration is not employed.

For comparison similar calculations were carried out for the CN-Scheme and the explicit Runge–Kutta method (the RK4-method) [40], which are of the second and fourth orders of accuracy, respectively. For the method RK4, values of the

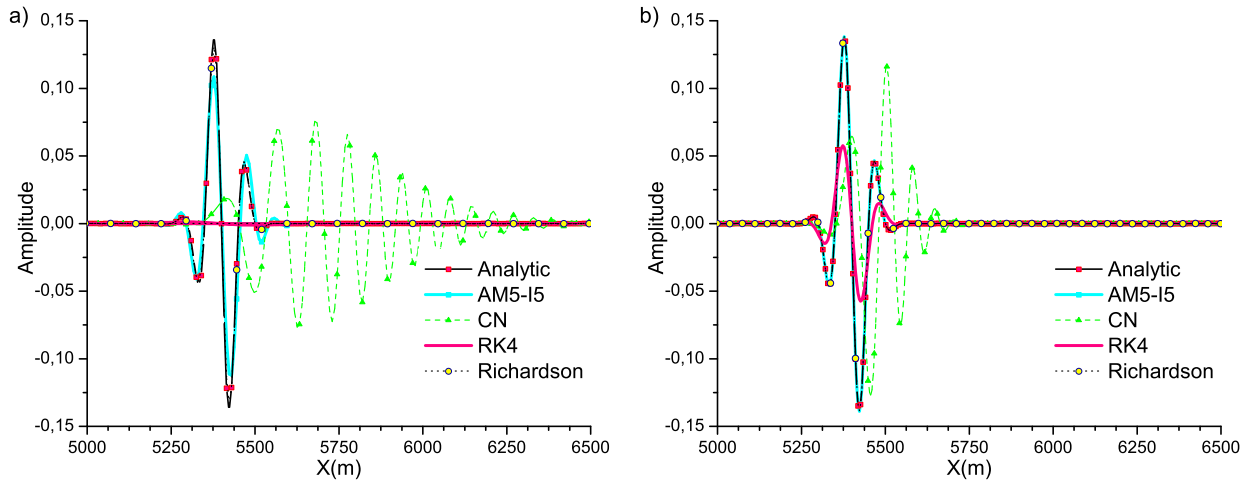

Fig. 1. Dependence of the wave field on the coordinate for the method proposed and different meshes (a) $N_x = 1000$, (b) $N_x = 2000$.

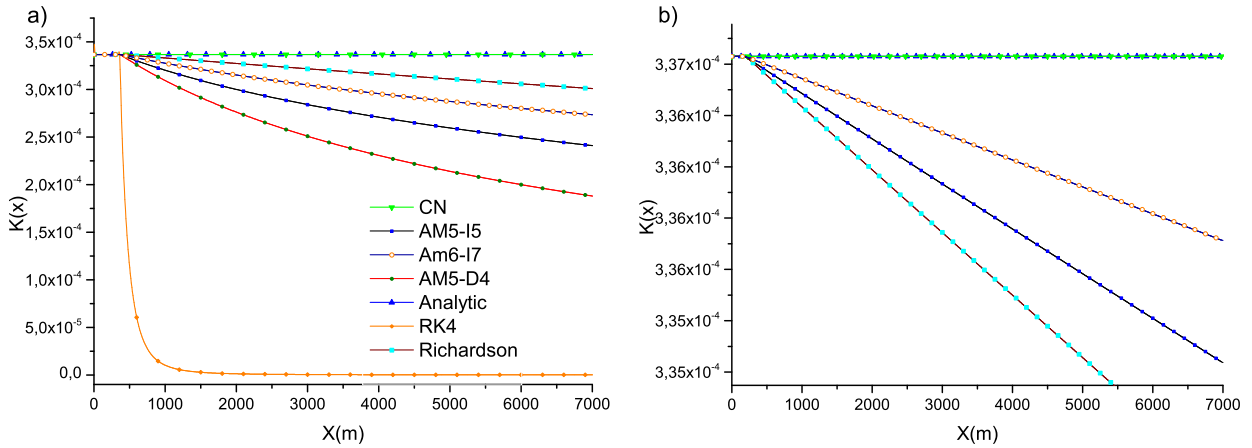

Fig. 2. Dependence of the value $K(x)$ on the coordinate for different methods and meshes: (a) $N_x = 1000$, (b) $N_x = 2000$. (For interpretation of the colors in the figure(s), the reader is referred to the web version of this article.)

grid function $\Phi_1\left(\bar{v}^m\right)$ in semi-integer nodes of the mesh were calculated with the quintic splines. The implementation of the implicit Runge–Kutta method of a high-order is not reasonable because of essentially higher computer costs as compared to the approaches proposed in the given study. From Table 1 and Fig. 1 it is clear that the method RK4 and the CN-scheme are stable and converge to the analytical solution with decreasing the mesh size. However for large mesh steps, the method RK4 possesses a pronounced numerical dissipation, while on the contrary, the Crank–Nicolson scheme demonstrates the dispersive error. A low accuracy for the large mesh steps makes the application of these algorithms disadvantageous in comparison with the Adams methods.

To evaluate the dissipative properties of the methods proposed, let us consider the integral of the form

$$K(x) = \int_0^\infty v^2(x,t)dt = \sum_{k=0}^{\infty}\left[\bar{v}^k(x)\right]^2, \tag{25}$$

where the latter equality is the Parseval relation.

For problem (3), (15) at $c = const > 0$ with a sufficient number of terms in Laguerre series (4), $K(x) = const$ should hold with a good accuracy. Figs. 2a, b show that for the analytical method (22), (23) and for the CN-scheme the value $K(x)$ is preserved with the precision of a machine. However due to the numerical dispersion the solution obtained with the CN-scheme does not satisfy the 1D OWWE equation with some kind of accuracy for large mesh steps. The Richardson method at $N_x = 1000$ (Fig. 2a) is less dissipative than the algorithms AM5-I5 and AM6-I7, while with an increase of the number of mesh nodes (Fig. 2b) the situation is contrary. This means that when solving the 2D OWWE by the Richardson method the stability will be stronger as compared to the Adams methods. The method RK4 is most dissipative among all under consideration, hence, the initial impulse from the source has smoothed into the straight line (Fig. 1a). Thus, the

explicit method RK4 and the CN-scheme, as was already mentioned, cannot be offered for the use within the Laguerre method.

6. The 2D one-way wave equation solver

6.1. Temporal approximation

Let us write down 2D OWWE (1), (2) for the spatial-temporal domain [13,14]

$$\begin{cases} \dfrac{\partial u}{\partial t} + c\dfrac{\partial u}{\partial z} - \displaystyle\sum_{s=1}^{n} \dfrac{\partial \psi_s}{\partial t} = 0, \quad \text{(a)} \\ \dfrac{1}{c^2}\dfrac{\partial^2 \psi_s}{\partial t^2} - \gamma_s \dfrac{\partial^2 \psi_s}{\partial x^2} - \beta_s \dfrac{\partial^2 u}{\partial x^2} = 0, \quad s = 1, 2, \ldots n, \quad \text{(b)} \end{cases} \tag{26}$$

where $u \equiv u(x, z, t)$ is the field variable, $\psi_s \equiv \psi_s(x, z, t)$ are auxiliary functions.

Assuming $g(0) = \frac{dg}{dt}(t)\Big|_{t=0} = 0$ and $\lim_{t\to\infty} g(t) = \lim_{t\to\infty} \frac{dg}{dt}(t) = 0$, we can show [34,41] that

$$L\left\{\frac{d^2}{dt^2} g(t)\right\} = \left(\frac{\eta}{2}\right)^2 \bar{g}_m + \Phi_2(\bar{g}_m), \quad \Phi_2(\bar{g}_m) \equiv \eta^2 \sum_{j=0}^{m-1} (m-j)\bar{g}_j.$$

Then applying the Laguerre transform (4) to equations (26) we obtain the following system of equations for the calculation of the m-th coefficient of expansion:

$$\begin{cases} \tilde{\eta}\bar{u}^m + c\dfrac{\partial \bar{u}^m}{\partial z} = \displaystyle\sum_{s=1}^{3} \left(\tilde{\eta}\bar{\psi}_s^m + \Phi_1\left(\bar{\psi}_s^m\right)\right) - \Phi_1\left(\bar{u}^m\right), \quad \text{(a)} \\ c^2\gamma_s \dfrac{\partial^2 \bar{\psi}_s^m}{\partial x^2} - \tilde{\eta}^2 \bar{\psi}_s^m + \beta_s c^2 \dfrac{\partial^2 \bar{u}^m}{\partial x^2} = \Phi_2(\bar{\psi}_s^m), \quad s = 1, 2, 3, \quad \text{(b)} \end{cases} \tag{27}$$

where $\tilde{\eta} = \eta/2$ and the index m denotes number of a term in series (4). The polynomial coefficients γ_s, β_s for $n = 3$ are chosen as follows: $\gamma_1 = 0.972926132$, $\gamma_2 = 0.744418059$, $\gamma_3 = 0.150843924$, $\beta_1 = 0.004210420$, $\beta_2 = 0.081312882$, $\beta_3 = 0.414236605$, for which, as shown in [5,15], such approximation is valid up to the angles of 89 degrees.

6.2. The spatial approximation

Multistep schemes of the Adams type of a high-order for solving the 2D OWWE are of practical importance as opposed to the Richardson method which requires solving an auxiliary problem on the mesh Ω_2 with a doubled number of the nodes. To approximate equation (27) we will use the Adams–Moulton scheme of the fifth order of accuracy:

$$\begin{cases} \dfrac{\bar{u}_{ik+1}^m - \bar{u}_{ik}^m}{h_z} = \dfrac{1}{720c} \displaystyle\sum_{j=-3}^{1} \alpha_j \left(\sum_{s=1}^{3} \left(\tilde{\eta}\bar{\psi}_{ik+j}^{m,s} + \Phi_1\left(\bar{\psi}_{ik+j}^{m,s}\right)\right) - \tilde{\eta}\bar{u}_{ik+j}^m - \Phi_1\left(\bar{u}_{ik+j}^m\right)\right), \quad \text{(a)} \\ c^2\gamma_s \mathcal{L}_x \bar{\psi}_{ik+1}^{m,s} - \tilde{\eta}^2 \bar{\psi}_{ik+1}^{m,s} = -c^2\beta_s \mathcal{L}_x \bar{u}_{ik+1}^m + \Phi_2(\bar{\psi}_{ik+1}^{m,s}), \quad s = 1, 2, 3, \quad \text{(b)} \end{cases} \tag{28}$$

where the coefficients of the difference scheme $\alpha_{-3} = -19$, $\alpha_{-2} = 106$, $\alpha_{-1} = -264$, $\alpha_0 = 646$, $\alpha_1 = 251$ and the difference operator $\mathcal{L}_x$ is of the form

$$\mathcal{L}_x f(x) \equiv \frac{1}{h_x^2}\left[a_0 f(x) + \sum_{j=1}^{N} a_j \left(f(x - jh_x) + f(x + jh_x)\right)\right] = \frac{\partial^2 f}{\partial x^2}(x) + O\left(h_x^{2N}\right). \tag{29}$$

For approximating $\partial^2/\partial x^2$ it is reasonable to use the dispersion-relationship-preserving method (DRP) by Tam and Webb [36], for which according to the Fourier derivative rule, $k_j \Longleftrightarrow -\mathrm{i}\partial_j$, values of the optimized coefficients a_n in formula (29) are defined as solution to the problem of minimizing the error functional in the space of wave numbers. This approach and its various modifications [50–52] make it possible to decrease the number of the mesh nodes and to preserve high accuracy of calculations as compared to conventional difference schemes obtained with the Taylor expansion in series [45]. To provide the twelfth approximation order the coefficients of difference scheme (29) were chosen as follows [52]: $a_0 = -3.12513824$, $a_1 = 1.84108651$, $a_2 = -0.35706478$, $a_3 = 0.10185626$, $a_4 = -0.02924772$, $a_5 = 0.00696837$, $a_6 = -0.00102952$.

6.3. The solution of the SLAEs

Let us write down the difference problem (28) in the form of a SLAE as

$$\begin{pmatrix} \gamma_1 c^2\mathcal{L}_x - \tilde{\eta}^2 I & 0 & 0 & \beta_1 c^2\mathcal{L}_x \\ 0 & \gamma_2 c^2\mathcal{L}_x - \tilde{\eta}^2 I & 0 & \beta_2 c^2\mathcal{L}_x \\ 0 & 0 & \gamma_3 c^2\mathcal{L}_x - \tilde{\eta}^2 I & \beta_3 c^2\mathcal{L}_x \\ -251/720\tilde{\eta} I & -251/720\tilde{\eta} I & -251/720\tilde{\eta} I & \left(c/h_z + 251/720\tilde{\eta}\right) I \end{pmatrix} \begin{pmatrix} \bar{\boldsymbol{\Psi}}^{m,1}_{k+1} \\ \bar{\boldsymbol{\Psi}}^{m,2}_{k+1} \\ \bar{\boldsymbol{\Psi}}^{m,3}_{k+1} \\ \bar{\mathbf{U}}^{m}_{k+1} \end{pmatrix}$$
$$= \begin{pmatrix} \Phi_2\left(\bar{\boldsymbol{\Psi}}^{m,1}_{k+1}\right) \\ \Phi_2\left(\bar{\boldsymbol{\Psi}}^{m,2}_{k+1}\right) \\ \Phi_2\left(\bar{\boldsymbol{\Psi}}^{m,3}_{k+1}\right) \\ c/hz\bar{\mathbf{U}}^{m}_{k} + 1/720\left(\sum_{i=-3}^{0}\alpha_i\left(\tilde{\eta}\boldsymbol{\Theta}^{m}_{k+i} + \Phi_1\left(\bar{\boldsymbol{\Theta}}^{m}_{k+i}\right)\right) + \alpha_1\Phi_1\left(\bar{\boldsymbol{\Theta}}^{m}_{k+1}\right)\right) \end{pmatrix}, \tag{30}$$

where $\bar{\boldsymbol{\Theta}}^{m}_{k} = -\bar{\mathbf{U}}^{m}_{k} + \sum_{s=1}^{3}\bar{\boldsymbol{\Psi}}^{m,s}_{k}$ and I is the unit matrix. Employing the Schur complement [53], the mesh functions $\bar{\mathbf{U}}^{m}_{k+1}$ can be calculated through the solution to the following reduced SLAE

$$\left[\left(c/h_z + \frac{251}{720}\tilde{\eta}\right) I + \frac{251}{720}\tilde{\eta}\sum_{s=1}^{3}\beta_s c^2\mathcal{L}_x\left(\gamma_s c^2\mathcal{L}_x - \tilde{\eta}^2 I\right)^{-1}\right]\bar{\mathbf{U}}^{m}_{k+1} = \bar{\mathbf{F}}^{m}_{u} + \sum_{s=1}^{3} M_s^{-1}\bar{\mathbf{F}}^{m}_{\psi_s}, \tag{31}$$

where

$$M_s = \frac{\gamma_s c^2}{\tilde{\eta}^2}\mathcal{L}_x - I,$$
$$\bar{\mathbf{F}}^{m}_{u} = c/hz\bar{\mathbf{U}}^{m}_{k} + \frac{1}{720}\left(\sum_{i=-3}^{0}\alpha_i\left(\tilde{\eta}\bar{\boldsymbol{\Theta}}^{m}_{k+i} + \Phi_1\left(\bar{\boldsymbol{\Theta}}^{m}_{k+i}\right)\right) + \alpha_1\Phi_1\left(\bar{\boldsymbol{\Theta}}^{m}_{k+1}\right)\right),$$
$$\bar{\mathbf{F}}^{m}_{\psi_s} = \Phi_2\left(\bar{\boldsymbol{\Psi}}^{m,s}_{k+1}\right)/\tilde{\eta}^2.$$

Making use of the matrix property [54] for (31) we have:

$$(B+I)^{-1}B = I - (B+I)^{-1}, \tag{32}$$

multiplying the equation by the matrix $M_1M_2M_3$ and taking into consideration the commutative property of $M_iM_j = M_jM_i$, we obtain the governing equation for the calculation of the mesh functions $\bar{\mathbf{U}}^{m}_{k+1}$

$$\left[M_1M_2M_3\left(c/h_z + \tilde{\eta} + \frac{251}{720}\tilde{\eta}\sum_{s=1}^{3}\frac{\beta_s}{\gamma_s}\right) I + \frac{251}{720}\tilde{\eta}\left(\frac{\beta_1}{\gamma_1}M_2M_3 + \frac{\beta_2}{\gamma_2}M_1M_3 + \frac{\beta_3}{\gamma_3}M_1M_2\right)\right]\bar{\mathbf{U}}^{m}_{k+1}$$
$$= M_1M_2M_3\bar{\mathbf{F}}^{m}_{u} + \tilde{\eta}\left(M_2M_3\bar{\mathbf{F}}^{m}_{\psi_1} + M_1M_3\bar{\mathbf{F}}^{m}_{\psi_2} + M_1M_2\bar{\mathbf{F}}^{m}_{\psi_3}\right). \tag{33}$$

As opposed to the Fourier transform, the coefficients of the Laguerre expansion in series (4) are dependent in a recurrent manner (27). Hence, for a fixed k for different m it is required to solve the SLAEs many times with the common real matrix and the different right-hand sides. Matrix (33) is banded and can be explicitly represented without calculation of the matrices M_s^{-1} thus allowing us to apply efficient algorithms for solving SLAEs based on LU-decomposition. For solving the SLAEs with banded matrices with a parallel algorithm, it is reasonable to use the parallel dichotomy algorithm [37,39,38], which was developed for tridiagonal matrices and block-tridiagonal matrices. The number of arithmetical operations, the dichotomy algorithm is comparable with other available algorithms; however the time needed for inter-process communications is considerably less for the dichotomy algorithm as compared to other algorithms. This is because the implementation of the dichotomy process on a supercomputer reduces to the summation of series. The commutative and associative properties of addition enable a considerable reduction in the total computation time with the use of inter-processor interaction optimization algorithms. After the calculation of the mesh functions $\bar{\mathbf{U}}^{m}_{k+1}$, before turning to calculating the functions $\bar{\mathbf{U}}^{m}_{k+2}$, the functions $\bar{\Psi}^{m,s}_{k+1}$ should be calculated as

$$M_s\bar{\boldsymbol{\Psi}}^{m,s}_{k+1} = \tilde{\eta}^{-2}\left(-\beta_s c^2\mathcal{L}_x\bar{\mathbf{U}}^{m}_{k+1} + \Phi_2\left(\bar{\boldsymbol{\Psi}}^{m,s}_{k+1}\right)\right),\ s = 1,2,3. \tag{34}$$

Making use of equality (32), we arrive at

$$\bar{\Psi}_k^{m,s} = M_s^{-1}\left(-\frac{\beta_s}{\gamma_s}\bar{\mathbf{U}}_k^m + \frac{1}{\tilde{\eta}^2}\Phi_2\left(\bar{\Psi}_k^{m,s}\right)\right) - \frac{\beta_s}{\gamma_s}\bar{\mathbf{U}}_k^m, \quad s = 1, 2, 3. \tag{35}$$

For solving the 2D OWWE, the stabilization of both the numerical instability of difference approximation for the operator $\partial/\partial z$ and the instability of the real Padé approximation (2) is need. The method AM5-I5 allows solving these problems.

Algorithm 2-1. The Adams–Moulton downward-continuation procedure for the 2D OWWE.

To calculate the mesh functions $\bar{\mathbf{U}}^m$, $\bar{\Psi}^m$ accurate to $O(h_x^{\xi} + h_z^5)$, the following is necessary:

1. Let the number of nodes of the mesh Ω in the direction z be odd. For all i for the functions $\Phi_1(\bar{u}_{ik}^m)$, $\Phi_2(\bar{\psi}_{ik}^{m,s})$ construct, independently, the 1D quintic splines [44] in the direction z, using only odd values of k.
2. Replace the values of the functions $\Phi_1(\bar{u}_{ik}^m)$, $\Phi_2(\bar{\psi}_{ik}^{m,s})$ for even k by their interpolated values (the quintic spline filtration).
3. For $k = 4, \ldots, K-1$
   3.1. Applying equation (33), calculate the solution $\bar{\mathbf{U}}_{k+1}^m$.
   3.2. Applying equation (34), calculate the solution $\bar{\Psi}_{k+1}^{m,s}$, $s = 1, 2, 3$.
4. Turn to the calculation of the $(m+1)$th, the $(m+2)$th, etc. coefficients of the Laguerre series expansion.

The above-considered way of stabilizing the solution allows the stability not only of the Adams–Moulton implicit schemes, but also of the Adams–Bashfort explicit schemes that are stable for the essentially lesser steps h_z. As consequence, the number of SLAEs to be solved in the form (33), (34) is multiply increased thus making the Adams–Bashfort method inefficient. Let us now consider the predictor–corrector method combining the computational efficiency of explicit and high stability of the implicit Adams schemes.

For equation (27a) as a predictor procedure we choose the Adams–Bashfort explicit method of the fifth order of accuracy

$$\frac{\bar{u}_{ik+1}^m - \bar{u}_{ik}^m}{h_z} = \frac{1}{720c}\sum_{j=-4}^{0}\varrho_j\left(\sum_{s=1}^{3}\left(\tilde{\eta}\bar{\psi}_{ik+j}^{m,s} + \Phi_1\left(\bar{\psi}_{ik+j}^{m,s}\right)\right) - \tilde{\eta}\bar{u}_{ik+j}^m - \Phi_1\left(\bar{u}_{ik+j}^m\right)\right), \tag{36}$$

where $\varrho_0 = 1901$, $\varrho_{-1} = -2774$, $\varrho_{-2} = 2616$, $\varrho_{-3} = -1274$, $\varrho_{-4} = 251$. In terms of correction we will use the Adams–Moulton scheme of the fifth order of accuracy (28a), where unknown values $\bar{\psi}_{ik+1}^{m,s}$ should be replaced by predicted values. In this case, the functions $\bar{u}_{ik+1}^m$ are explicitly expressed. If for the correction we use scheme (28a) and substitute the predicted values both for $\bar{\psi}_{ik+1}^{m,s}$, and for $\bar{u}_{ik+1}^m$ into the right-hand side, then for the sake of stability, smaller steps h_z and, simultaneously, a larger number of corrections will be required.

Algorithm 2-2. The Predictor–Corrector downward-continuation procedure for the 2D OWWE.

To calculate the mesh functions $\bar{\mathbf{U}}^m$, $\bar{\Psi}^m$ accurate to $O(h_x^{\xi} + h_z^5)$, the following is necessary:

1. Let the number of nodes of the mesh Ω in the direction z be odd. For all i for the functions $\Phi_1(\bar{u}_{ik}^m)$, $\Phi_2(\bar{\psi}_{ik}^{m,s})$ independently construct the 1D quintic splines [44] in the direction z using only odd values of k.
2. Replace values of the functions $\Phi_1(\bar{u}_{ik}^m)$, $\Phi_2(\bar{\psi}_{ik}^{m,s})$ for even k by their interpolated values (the quintic spline filtration).
3. For $k = 4, \ldots, K-1$
   3.1. Applying equation (36), calculate the predicted solution $\breve{\mathbf{U}}_{k+1}^m$.
   3.2. Applying equation (35) with $\breve{\mathbf{U}}_{k+1}^m$, calculate the predicted solution $\breve{\Psi}_{k+1}^{m,s}$, $s = 1, 2, 3$.
   3.3. Applying equation (28a), substituting $\breve{\Psi}_{k+1}^{m,s}$ instead of $\bar{\Psi}_{k+1}^{m,s}$, calculate the corrected solution $\breve{\breve{\mathbf{U}}}_{k+1}^m$.
   3.4. Applying equation (35) with $\breve{\breve{\mathbf{U}}}_{k+1}^m$, calculate the final solution for $\bar{\Psi}_{k+1}^{m,s}$, $s = 1, 2, 3$.
   3.5. Applying equation (28a) with $\bar{\Psi}_{k+1}^{m,s}$, calculate the final solution for $\bar{\mathbf{U}}_{k+1}^m$.
4. Turn to the calculation of the $(m+1)$th, the $(m+2)$th, etc. coefficients of the expansion of the Laguerre series.

Thus, instead of indefinite non-symmetrical SLAE (33) it is necessary to solve SLAEs of the form (35) with sign-defined symmetric matrices of lesser dimensions resulting in the use of efficient algorithms of the computational linear algebra and a decrease in the calculation time. As compared to the Marchuk–Strang method that is accurate to the second order [24], the predictor–corrector method is of the fifth order of accuracy. Further increase of approximation order is not reasonable because for providing the stability an essentially smaller step h_z should be set.

Both for the Adams method and for the predictor–corrector method one needs initial values to start the calculation. For obtaining such initial values, it is required to use other methods such as the Richardson extrapolation or Crank–Nicolson scheme with a smaller step.

7. Numerical experiments for the 2D one-way wave equation

Analytically it is really difficult to provide a strict mathematical substantiation of algorithms of a high-order of accuracy for the 2D OWWE. Therefore to confirm the efficiency of the approaches proposed, thorough testing is needed. Let us discuss

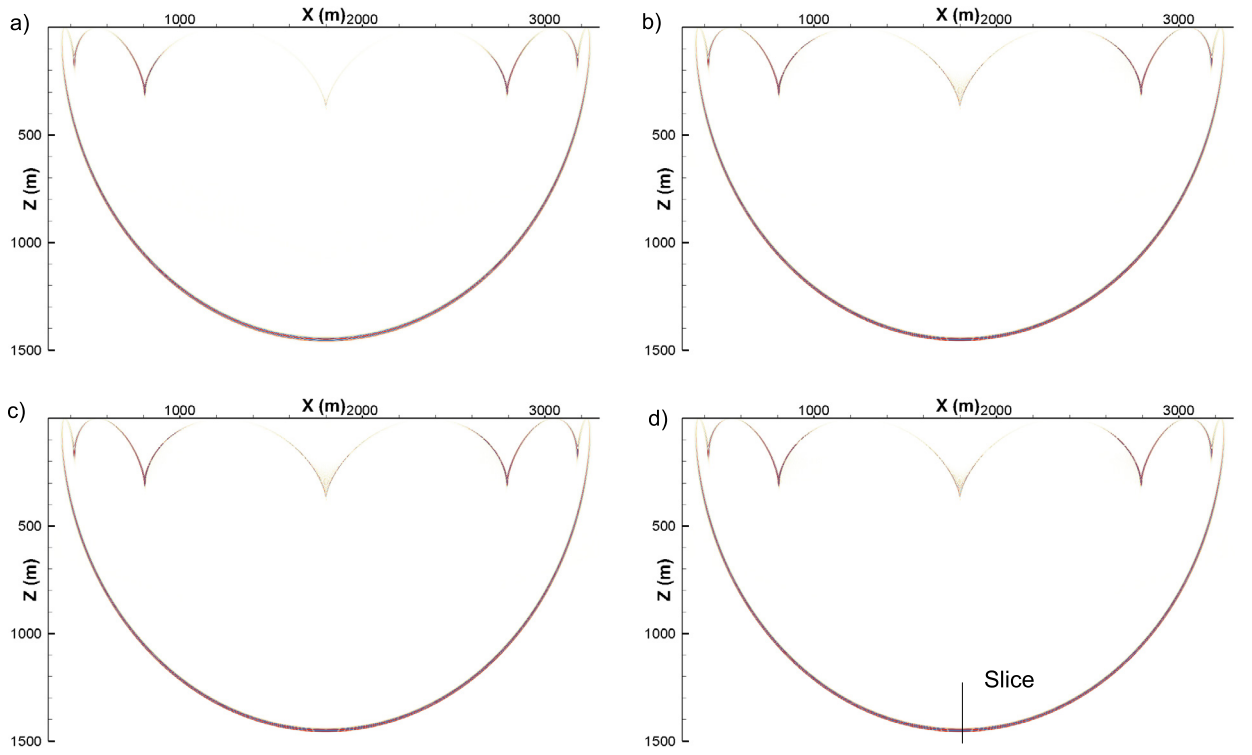

Fig. 3. Snapshots for the wave field at $t = 6$ s for the homogeneous velocity model. (a) The Richardson extrapolation $h_{x,z} = 1$ m and (b) $h_{x,z} = 0.5$ m, (c) AM5-I5 method with $h_x = 1$ m, $h_z = 0.3$ m, (e) PC5-I5 method with $h_x = 1$ m, $h_z = 0.3$ m.

a few tests that would allow the evaluation of the quality of the solution to be obtained as compared with the Richardson algorithm. Numerical procedures were implemented in Fortran-90 using the MPI library.

7.1. The impulse response for homogeneous media

In the first test we illustrate analyzing the accuracy by the impulse responses. For the calculation, we used the homogeneous medium model with the velocity 250 m/s and the size 3.5 km × 1.5 km. The point source (24) with the parameters $t_0 = 0.2s$, $\delta = 4$, $f_0 = 30$ Hz was located at the center of the upper surface. The number of addends in series (4) was $n = 2500$ for $T = 6$ s; the expansion parameter was $\eta = 600$.

A disadvantage of the Laguerre transform is the absence of the fast transformation algorithm. The implementation of the forward Laguerre transform (4) with the help of the method of least squares, the number of arithmetical operations will be of order $O(NP)$, where P is the number of discrete points of an approximated function and $N \leq P$ is the number of terms in the Laguerre series needed for attaining the required accuracy in the norm L_2, whereas for the fast Fourier transform computer costs are essentially less and make up $O(N \log(N))$. However, taking into account the fact that input data are set only along the upper surface ($z = 0$), and the inverse transformation is done for a fixed time instant, the total cost of the direct and inverse transformations appears to be minor as compared to that needed for the calculation of coefficients of series (4) from the solution to problem (27). The numerical experiments have confirmed that the time needed for carrying out the Laguerre transform for the initial data is less than one percent of the total calculation time. Supplementary aspects as regards carrying out the Laguerre transform and the basis functions are considered in [55–57].

In Section 5, for the 1D OWWE it was shown that with an equal mesh size the Richardson extrapolation is more accurate than the AM5-I5-scheme, which is also valid for the 2D case. If one selects the step $h_z = 1$ m for the mesh Ω_1 for the Richardson method and the step $h_z = 0.3$ m for the AM5-15 and PC5-15 methods, then the whole volume of calculations and calculation accuracy for all the three methods will be compatible (Fig. 3). However with a thorough consideration of values of the amplitudes along the straight line “Slice” it appears to be clear (Fig. 4a) that the AM5-I5 and the PC5-I5 methods are more accurate when the number of nodes of the mesh Ω is equal to the number of nodes of the meshes Ω_1, Ω_2.

A considerable accuracy and computational efficiency of the AM5-I5, PC5-I5 methods are attained at the expense of a lesser stability as compared to the Richardson method. It was experimentally revealed that for the Richardson method the condition of stability is of the form $h_z/h_x \leq 1$, while for the AM5-I5 method it should be $h_z/h_x < 0.4$, and for the PC5-I5 algorithm the stability is attained at $h_z/h_x < 0.3$. The fact that minimum steps required for providing a good accuracy and

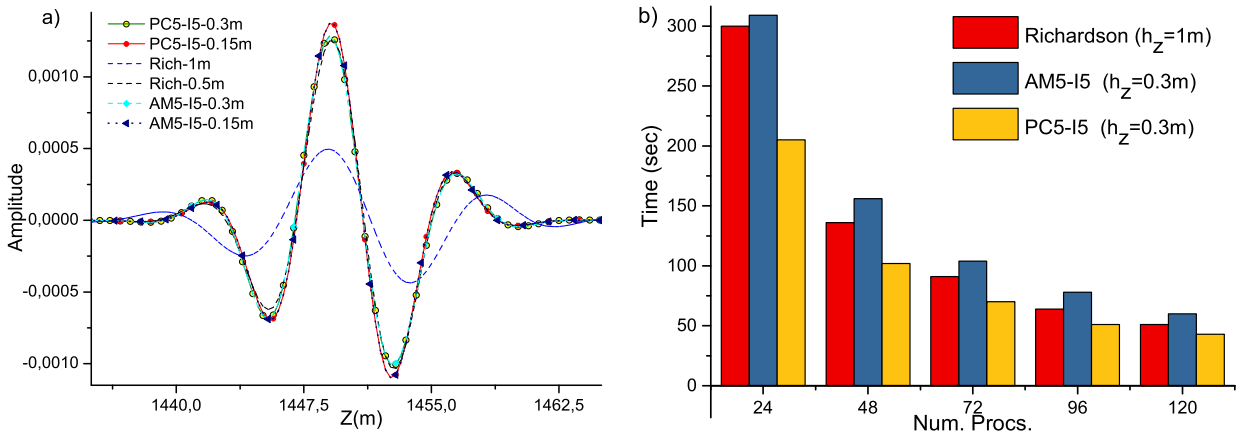

Fig. 4. (a) Dependence of the wave field on the coordinate along the straight line "Slice" (Fig. 3) for different meshes and methods. (b) Dependence of the time of computing the test "Impulse response" on the number of CPU cores for the different methods.

stability almost coincide, allows us to propose the statement about the balance of the PC5-I5 method which is by 20–30% more efficient as compared to the AM5-I5 method (Fig. 4b).

Additionally we have considered the AM6-I7 and the AM5-D4 methods, which are stable for the 1D OWWE but unstable for the 2D OWWE. This is because in addition to the numerical instability due to the choice of approximation for the operator $\partial/\partial z$, there is instability caused by the presence of a singular component in the solution to the OWWE, i.e. when denominators (2) are close to zero or vanish. In the AM5-D4 method, to approximate $\partial/\partial z$ different difference schemes were used for the right-hand and the left-hand sides of equations (7), (8). This approach stipulates an additional numerical dissipation, but does not allow restricting the growth of the number of singular components for the 2D OWWE. Also, the AM6-I7 method demonstrates (Fig. 2) the lesser dissipation as compared to the algorithm AM5-I5 and, hence, insufficient level of fictitious absorption does not allow stabilizing the numerical scheme.

7.2. The impulse response for inhomogeneous media

Equation (1) was obtained for a homogeneous medium, but the calculations can be made for inhomogeneous media as well. In this case one should take into account that the approximation (2) for the real coefficients γ_s and β_s may be unstable, especially for models with abrupt changes in the velocities [13,14]. One of the reasons of this instability is that the denominator of (2) can take values very close to zero. This increases considerably the corresponding Fourier-components of the solution. Also, for negative subradical values the approximation (2) is inconsistent for the real coefficients γ_s and β_s. Actually, the expression in the left-hand side of (2) may take a complex value, whereas that in the right-hand side is always real. Although the spline-filtering algorithm limits the growth of unstable Fourier components of the solution, the discontinuous velocity model has to be smoothed prior to the calculations. To restrict numerical instability one can use a simple Gaussian or box filter [58]. In general, these filters act as lowpass frequency filters and, therefore, can reduce the spatial intensity derivatives present in the velocity model. Consider a test for the inhomogeneous velocity models in Fig. 5b and Figs. 6a, b. The parameters for the calculation are taken as in the previous test with the homogeneous velocity model. The velocity models are pre-smoothed using the Gaussian blur filter with a 3×3 kernel. For the models in Fig. 5a and Fig. 6a, it was sufficient to use the smoothing filter once, whereas for the model in Fig. 6b, with higher velocity gradients, the filter had to be used three times. The number of smoothing iterations can be decreased when using a larger filter kernel, for instance, 5×5 or 7×7.

One can see from Fig. 5 that the algorithm based on the Richardson method [32] has the greatest dissipation, and the AM5-I5 method, the least dissipation. This explains higher stability of the method [32], which does not require pre-smoothing for this velocity model, whereas the amplitude variations in the waves of interest to us are greater than those calculated by the AM5-I5 and PC5-I5 methods. The AM5-I5 and PC5-I5 methods are comparable in accuracy. In this case the calculation time of the PC5-I5 method is minimal and corresponds to that of the homogeneous velocity model test (Fig. 4b). The same calculation times of the two tests can be explained by the fact that the presence of inhomogeneity in the medium when using direct methods to solve the SLAEs does not affect the efficiency of the method on the whole. In the calculations with larger velocity gradients (see Figs. 6a, b) there appear additional nonphysical waves (denoted by arrows). The larger is the local contrast of the medium, the greater is the amplitude of the fictitious wave, and its propagation speed is much less than that of the medium, which agrees with the theory [13,14]. This test has shown that with the spline filtering procedure both the initially unstable operator and the multistep schemes can be stabilized, whereas good conditionality of the SLAEs and high accuracy of the method on the whole can be preserved.

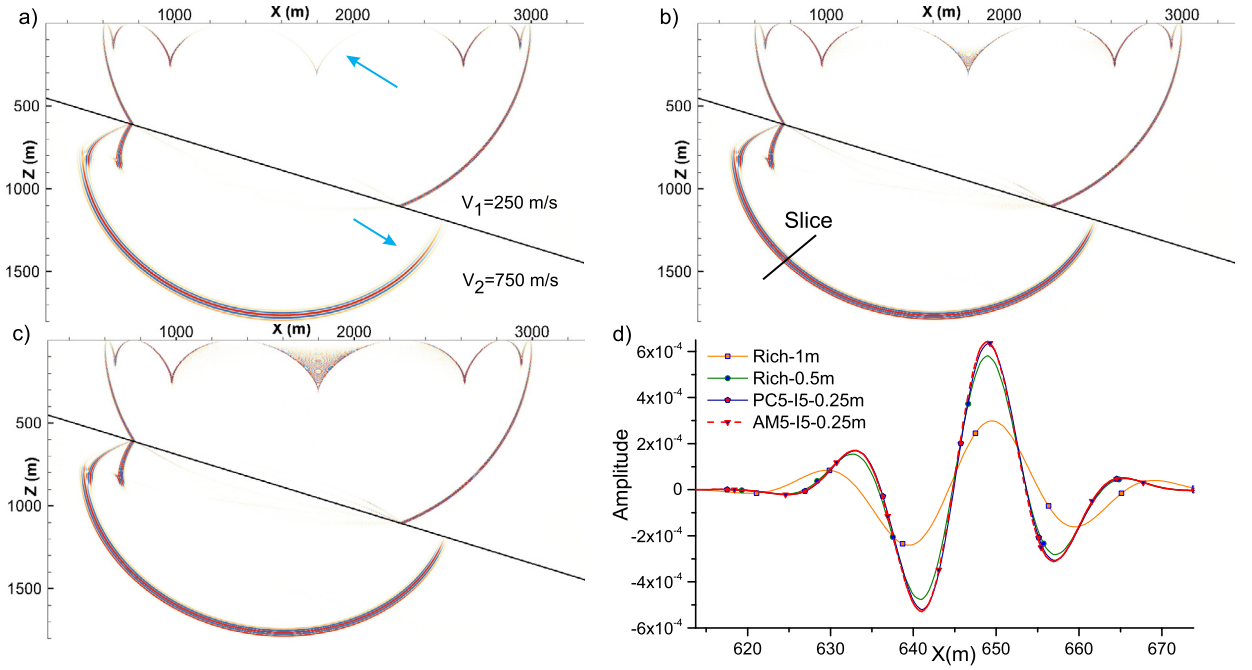

Fig. 5. Snapshots for the wave field at $t = 5$ s for the inhomogeneous velocity model. (a) The Richardson extrapolation $h_{x,z} = 1$ m, (b) PC5-I5 method with $h_x = 1$ m, $h_z = 0.25$ m, (c) AM-I5 method with $h_x = 1$ m, $h_z = 0.25$ m. (d) Dependence of the wave field on the coordinate along the straight line "Slice" (Fig. 5b) for different methods and h_z with $h_x = 1$. High energy dissipation of the wave field is shown by arrows.

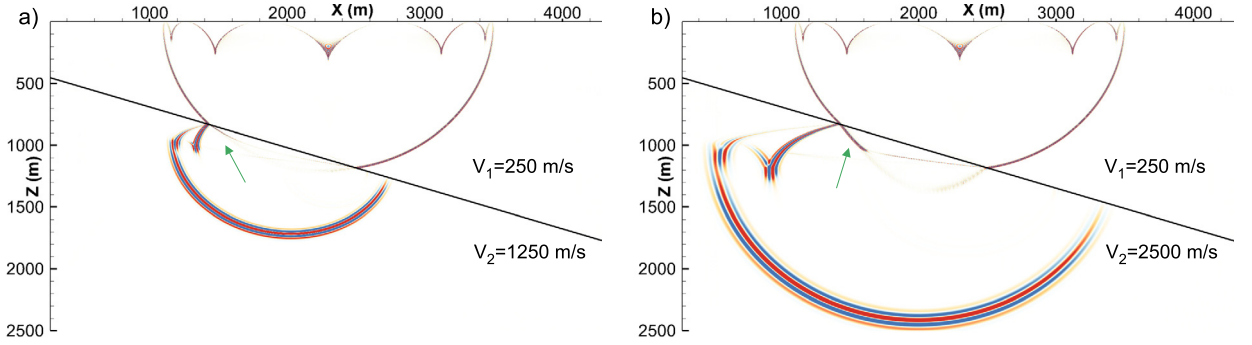

Fig. 6. Snapshots for the wave field at $t = 5$ s for the different inhomogeneous velocity models for the PC5-I5 method with $h_x = 1$ m, $h_z = 0.25$ m. A nonphysical wave caused by a large velocity difference at the interface between the two media is shown by arrows.

7.3. Migration procedures

From a mathematical point of view, the migration operator is a linear operator focusing every scattered wave to a scattering point. In other words, we change from preliminarily processed seismograms to an in-depth image of the medium. This is done to exclude the undesirable geometrical effects of wave propagation for subsequent estimation of the medium's properties using an observed seismic signal passing through the medium. Migration, known as post-stack migration, was introduced by J.F. Claerbout within the framework of the model of exploding boundaries [4]. The migration algorithms have been extensively developed in the last fifty years (in particular, more precise algorithms of pre-stack migration have been created [59,60]). Nevertheless, to test the algorithm proposed for solving the OWWE equation we consider only post-stack migration, which will be sufficient for estimating the stability and accuracy of the developed procedures. Such calculations were performed in [32] to test the algorithm based on a combination of the Laguerre transform and the Richardson extrapolation. As compared to the Finite Difference (FD) [11], Fourier Finite Difference (FFD) [16] and Phase Shift Plus Interpolation (PSPI) [61] methods, the algorithm of [32] has made it possible to obtain a more precise solution. Let us now consider a similar test for the algorithms AM5-I5, PC5-I5 to solve the 2D OWWE.

Theoretical seismograms (Fig. 7b) for the syncline model (Fig. 7a) were obtained with the help of the Gaussian beams algorithm [62,63] implemented in the package Seismic Unix. For setting the boundary condition on the upper surface, the function for the zero-offset section $u(x, z, t)|_{z=0} = g(x, t)$ was expanded in series (4) with the parameters $n = 2500$ and

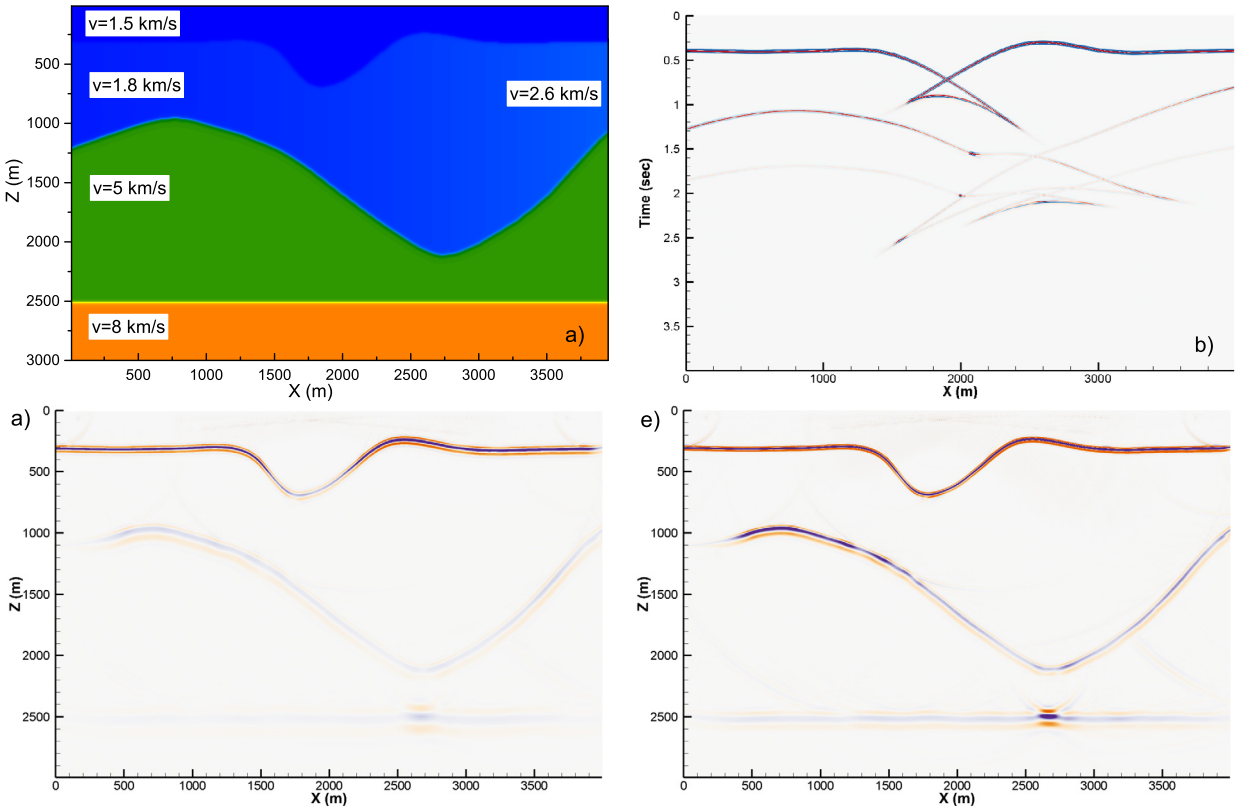

Fig. 7. (a) Syncline model and (b) zero-offset section. Snapshots for the wave field at $t = 4$ s (c) for the Richardson extrapolation $h_x = h_z = 6$ m, (d) for the AM5-I5 and PC5-I5 methods $h_x = 6$ m, $h_z = 3$ m.

$\eta = 800$ for $t \in [0, 4]$ s. The calculations were carried out on the meshes with the steps $h_x = 6$ m, $h_z = 3$ or 6 m for the Richardson method $h_x = 6$ m and $h_z = 3$ or 1 m for the methods AM5-I5, PC5-I5. According to the model of explosive boundaries, the velocities were set to be half the true velocity of the medium model. The model in Fig. 7a was preliminarily smoothed by using the Gaussian blur filter with a 3×3 kernel, since otherwise for the algorithms AM5-I5 and PC5-I5 there emerges instability on the interface between the two media. A smooth velocity function is required by most migration algorithms, since the use of a smoothed velocity model usually gives more stable results with a smaller number of artifacts in the image. Another argument for smoothing is that when solving practical problems of seismic prospecting it is rather difficult to exactly determine the locations of discontinuities for a velocity model of the medium. In this case smoothing is a natural technique, since it minimizes the error in specifying the function of the medium in some norm. The choice of a procedure and a degree of smoothing depends both on a migration algorithm and a model of the medium. Some questions of the effects of the smoothing scale of the function are discussed in [64,65].

In Figs. 7c, d it is clear that the Richardson extrapolation is less accurate if the general number of nodes of the meshes Ω_1, Ω_2 is equal to the number of nodes of the mesh Ω for the methods AM5-I5, PC5-I5. If the mesh steps are equal to one another, the quality of the image obtained is approximately the same, but the Richardson method requires three times as many calculations as compared to other techniques. The algorithms AM5-I5 and PC5-I5 (Fig. 7d) allow obtaining images that are of the same accuracy, which witnesses to the correctness of calculations because different ideas of using the Adams schemes underlie these methods. The spline-filtration procedure makes it possible to provide the stability with lesser costs than the Richardson extrapolation and the method PC5-I5 is three times more efficient than the method AM5-I5.

8. Conclusion

As a result, determining the reasons of the numerical instability for the schemes of high-orders of accuracy in solving the OWWE have allowed us to propose the stabilizing procedure based on the spline-filtration and as consequently to implement the Adams multistep schemes and the predictor–corrector method accurate to the fifth order. A combination of the Laguerre transform and the predictor–corrector method reduces the original problem to solving the SLAEs with symmetrical well-conditioned real matrices, that is one of the main advantages of the methods proposed as compared to the classical Fourier approach. In the 2D case, the direct algorithms for solving SLAEs are applied, which are less sensitive to the above-mentioned properties of matrices. For the case of the 3D problems, the conditioning of matrices defines the rate of convergence of iterative procedures and, hence, the total calculation time.

In spite of the fact that the Richardson extrapolation procedure demands higher computer costs than the Adams multistep methods, one should not completely reject its application. First, the Richardson method possesses a greater numerical dissipation, which in many cases makes it possible to calculate inhomogeneous velocity models without preliminary smoothing. Also, supplementary stability will not be redundant when considering the OWWE for an elastic model. Second, the Richardson method can be used to calculate the initial values for multistep methods that are not self-starting. As a rule, for solving this problem the Runge–Kutta type schemes are employed, but within the Laguerre method such schemes do not provide the required accuracy due to the strong numerical dissipation.

A combination of the spline-filtration, the Adams multistep methods and the Laguerre transform is mutually complementary. Experimentally it was verified that the change of the Adams methods for the backward difference schemes does not provide the stability of calculation with the help of the proposed stabilizing procedures, whereas the change of the Laguerre transform for the Fourier transform with respect to time makes the spline-filtration unreasonable. This is because in this case the solution for each harmonic is independently determined by the initial conditions on the daily surface. On the contrary, the matter of coefficients of the Laguerre series and their recurrent dependence make it possible to delicately remove unstable components of the wave field without new numerical artifacts. Thus, the considered ways of decreasing computer costs make the proposed methods of solving the OWWE to be promising for the calculation of applied problems.

Acknowledgements

The calculation was performed on the supercomputers of the Moscow and the Novosibirsk State Universities and of the Siberian Supercomputer Center. The work was supported by a grant from the Russian Ministry of Education no. MK-152.2017.5 and by Russian Foundation for Basic Research and the government of the Novosibirsk region of the Russian Federation, grant no. 18-41-543002.

References

[1] F.D. Tappert, The parabolic approximation method, in: Wave Propagation and Underwater Acoustics, Springer, Berlin, Heidelberg, 1977, pp. 224–287.
[2] F.B. Jensen, W.A. Kuperman, M.B. Porter, H. Schmidt, Computational Ocean Acoustics, Springer-Verlag, New York, 2011.
[3] D. Lee, A.D. Pierce, Er-C. Shang, Parabolic equation development in the twentieth century, J. Comput. Acoust. 08 (04) (2000) 527–637.
[4] J.F. Claerbout, Toward a unified theory of reflector mapping, Geophysics 36 (3) (1971) 467–481.
[5] O. Yilmaz, S.M. Doherty, Seismic Data Analysis: Processing, Inversion, and Interpretation of Seismic Data, Society of Exploration Geophysicist, 2001.
[6] D.A. Angus, The one-way wave equation: a full-waveform tool for modeling seismic body wave phenomena, Surv. Geophys. 35 (2) (2013) 359–393.
[7] B. Biondi, 3D Seismic Imaging, Society of Exploration Geophysicists, 2006.
[8] E.L. Lindman, “Free-space” boundary conditions for the time dependent wave equation, J. Comput. Phys. 18 (1) (1975) 66–78.
[9] B. Engquist, A. Majda, Absorbing boundary conditions for the numerical simulation of waves, Math. Comput. 31 (1977) 629–651.
[10] L.N. Trefethen, L. Halpern, Well-posedness of one-way wave equations and absorbing boundary conditions, Math. Comput. 47 (176) (1986) 421–435.
[11] J.F. Claerbout, Imaging the Earth’s Interior, Blackwell Scientific Publications, Inc., Cambridge, MA, USA, 1985.
[12] L. Halpern, L.N. Trefethen, Wide-angle one-way wave equations, J. Acoust. Soc. Am. 84 (4) (1988) 1397–1404.
[13] A. Bamberger, B. Engquist, L. Halpern, P. Joly, Higher order paraxial wave equation approximations in heterogeneous media, SIAM J. Appl. Math. 48 (1) (1988) 129–154.
[14] A. Bamberger, B. Engquist, L. Halpern, P. Joly, Parabolic wave equation approximations in heterogenous media, SIAM J. Appl. Math. 48 (1) (1988) 99–128.
[15] M.W. Lee, S.Y. Suh, Optimization of one-way wave equations, Geophysics 50 (10) (1985) 1634–1637.
[16] D. Ristow, T. Rühl, Fourier finite-difference migration, Geophysics 59 (12) (1994) 1882–1893.
[17] Z. Li, Compensating finite-difference errors in 3-d migration and modeling, Geophysics 56 (10) (1991) 1650–1660.
[18] C. Bunks, Effective filtering of artifacts for implicit finite-difference paraxial wave equation migration, Geophys. Prospect. 43 (2) (1995) 203–220.
[19] F.A. Milinazzo, C.A. Zala, G.H. Brooke, Rational square-root approximations for parabolic equation algorithms, J. Acoust. Soc. Am. 101 (2) (1997) 760–766.
[20] Y.Y. Lu, A complex coefficient rational approximation of 1+x, Appl. Numer. Math. 27 (2) (1998) 141–154.
[21] D. Yevick, D.J. Thomson, Complex Padé approximants for wide-angle acoustic propagators, J. Acoust. Soc. Am. 108 (6) (2000) 2784–2790.
[22] D. Amazonas, C. Costa, J. Schleicher, R. Pestana, Wide-angle FD and FFD migration using complex Padé approximations, Geophysics 72 (6) (2007) S215–S220.
[23] G.I. Marchuk, Some application of splitting-up methods to the solution of mathematical physics problems, Appl. Mat. 13 (2) (1968) 103–132.
[24] G.I. Marchuk, Handbook of numerical analysis, in: P.G. Ciarlet, J.L. Lions (Eds.), Handbook of Numerical Analysis, vol. 1, Elsevier Science Publishers BV, 1990, pp. 197–460.
[25] G. Strang, On the construction and comparison of difference schemes, SIAM J. Numer. Anal. 5 (3) (1968) 506–517.
[26] Y. Saad, Iterative Methods for Sparse Linear Systems, SIAM, 2003.
[27] G.H. Golub, C.F. Van Loan, Matrix Computations, 3rd ed., Johns Hopkins University Press, Baltimore, MD, USA, 1996.
[28] A.A. Samarskij, E.S. Nikalayev, Numerical Methods for Grid Equations, Birkhauser Verlag, 1989.
[29] O.G. Ernst, M.J. Gander, Why It Is Difficult to Solve Helmholtz Problems with Classical Iterative Methods, Springer, Berlin, Heidelberg, 2012, pp. 325–363.
[30] C.A.N. Costa, I.S. Campos, J.C. Costa, F.A. Neto, J. Schleicher, A. Novais, Iterative methods for 3D implicit finite-difference migration using the complex Pade approximation, J. Geophys. Eng. 10 (4) (2013) 045011.
[31] E. Becache, F. Collino, M. Kern, P. Joly, Two migration methods based on paraxial equations in a 3D heterogeneous medium, in: Proc. SPIE 2571, Mathematical Methods in Geophysical Imaging III, vol. 2571, 1995, pp. 55–66.
[32] A.V. Terekhov, The Laguerre finite difference one-way equation solver, Comput. Phys. Commun. 214 (2017) 71–82.
[33] D. Jackson, Fourier Series and Orthogonal Polynomials, Dover Books on Mathematics, Dover Publications, 2004.
[34] L. Debnath, D. Bhatta, Integral Transforms and Their Applications, second edition, Taylor & Francis, 2006.
[35] G.I. Marchuk, V.V. Shaidurov, Difference Methods and Their Extrapolations, Appl. Math., Springer, New York, NY, 1983.
[36] C.K.W. Tam, J.C. Webb, Dispersion-relation-preserving finite difference schemes for computational acoustics, J. Comput. Phys. 107 (2) (1993) 262–281.

[37] A.V. Terekhov, Parallel dichotomy algorithm for solving tridiagonal system of linear equations with multiple right-hand sides, Parallel Comput. 36 (8) (2010) 423–438.
[38] A.V. Terekhov, A fast parallel algorithm for solving block-tridiagonal systems of linear equations including the domain decomposition method, Parallel Comput. 39 (6–7) (2013) 245–258.
[39] A.V. Terekhov, A highly scalable parallel algorithm for solving Toeplitz tridiagonal systems of linear equations, J. Parallel Distrib. Comput. 87 (2016) 102–108.
[40] J.C. Butcher, Numerical Methods for Ordinary Differential Equations, 2nd edition, Wiley, 2008.
[41] B.G. Mikhailenko, Spectral Laguerre method for the approximate solution of time dependent problems, Appl. Math. Lett. 12 (1999) 105–110.
[42] J.G. Charney, R. Fjortoft, J. von Neumann, Numerical integration of the barotropic vorticity equation, Tellus 2 (4) (1950) 237–254.
[43] J. Crank, P. Nicolson, A practical method for numerical evaluation of solutions of partial differential equations of the heat-conduction type, Proc. Camb. Philos. Soc. 43 (1) (1947) 50–67.
[44] J.G. Herriot, C.H. Reinsch, Algorithm 507: procedures for quintic natural spline interpolation [e1], ACM Trans. Math. Softw. 2 (3) (September 1976) 281–289.
[45] G.I. Marchuk, Methods of Numerical Mathematics, Springer-Verlag, 1982.
[46] J.-P. Berrut, L. Trefethen, Barycentric Lagrange interpolation, SIAM Rev. 46 (3) (2004) 501–517.
[47] H.J. Nussbaumer, Fast Fourier Transform and Convolution Algorithms, Springer-Verlag, 1982.
[48] J. Keilson, W. Nunn, U. Sumita, The bilateral Laguerre transform, Appl. Math. Comput. 8 (2) (1981) 137–174.
[49] G.V. Konyukh, B.G. Mikhailenko, A.A. Mikhailov, Application of the integral Laguerre transforms for forward seismic modeling, J. Comput. Acoust. 09 (04) (2001) 1523–1541.
[50] W. Liang, Y. Wang, C. Yang, Determining finite difference weights for the acoustic wave equation by a new dispersion-relationship-preserving method, Geophys. Prospect. 63 (1) (2015) 11–22.
[51] C. Chu, P.L. Stoffa, Determination of finite-difference weights using scaled binomial windows, Geophysics 77 (3) (2012) W17–W26.
[52] J.-H. Zhang, Z.-X. Yao, Optimized explicit finite-difference schemes for spatial derivatives using maximum norm, J. Comput. Phys. 250 (2013) 511–526.
[53] R.W. Cottle, Manifestations of the Schur complement, Linear Algebra Appl. 8 (3) (1974) 189–211.
[54] H.V. Henderson, S.R. Searle, On deriving the inverse of a sum of matrices, SIAM Rev. 23 (1) (1981) 53–60.
[55] R. Malti, D. Maquin, J. Ragot, Bilateral decomposition of a time function into Laguerre series. Application to LTI system identification, J. Franklin Inst. 335 (5) (1998) 851–869.
[56] A. Gil, J. Segura, N.M. Temme, Efficient computation of Laguerre polynomials, Comput. Phys. Commun. 210 (2017) 124–131.
[57] J. Abate, G. Choudhury, W. Whitt, On the Laguerre method for numerically inverting Laplace transforms, INFORMS J. Comput. 8 (4) (1996) 413–427.
[58] E.R. Davies, Computer and Machine Vision, Fourth Edition: Theory, Algorithms, Practicalities, 4th edition, Academic Press, 2012.
[59] S.H. Gray, J. Etgen, J. Dellinger, D. Whitmore, Seismic migration problems and solutions, Geophysics 66 (5) (2001) 1622–1640.
[60] G. Schuster, Seismic Inversion, Society of Exploration Geophysicists, 2017.
[61] J. Gazdag, P. Sguazzero, Migration of seismic data by phase shift plus interpolation, Geophysics 49 (2) (1984) 124–131.
[62] M.M. Popov, A new method of computation of wave fields using Gaussian beams, Wave Motion 4 (1982).
[63] V. Cerveny, Gaussian beam synthetic seismograms, J. Geophys. 58 (1985) 44–72.
[64] Samuel H. Gray, Velocity smoothing for depth migration: how much is too much?, 2005, pp. 1055–1058.
[65] Karel Žáček, Smoothing the Marmousi Model, Birkhäuser Basel, Basel, 2002, pp. 1507–1526.